Supplemental Material

Urban greenhouse gas emissions from the Berlin area: A case study using airborne CO_2 and CH_4 in situ observations in summer 2018

T. Klausner[1*], M. Mertens[1], H. Huntrieser[1], M. Galkowski[2,3], G. Kuhlmann[4], R. Baumann[1], A. Fiehn[1], P. Jöckel[1], M. Pühl[1] and A. Roiger[1]

[1]Deutsches Zentrum für Luft- und Raumfahrt (DLR), Institut für Physik der Atmosphäre, Oberpfaffenhofen, Germany

[2]Max-Planck-Institut für Biogeochemie (MPI), Biogeochemische Systeme (BGC), Jena, Germany

[3]AGH University of Science and Technology, Faculty of Physics and Applied Computer Science, Kraków, Poland

[4]Empa, Swiss Federal Laboratories for Materials Science and Technology, Dübendorf, Switzerland

*Corresponding author: theresa.klausner@dlr.de

ADD DOI here after acceptance of the manuscript

March 10, 2020

List of Contents

Figure S1. Time series of CO_2, CH_4 and flight altitude for five research flights during July 2018.

Figure S2. Vertical profiles of the upward spiral at Tempelhofer Feld. The PBL depth (dashed black line) was determined from virtual potential temperature, static temperature and relative humidity.

Figure S3. Aerosol lidar measurements at Leipzig. The temporal evolution of the range-corrected signal at 1064 nm is shown. Available at http://polly.tropos.de/?p=lidarzeit&Ort=1&Jahr=2018. Accessed October 04, 2019. Further information can be found in Engelmann et al. (2016) and Baars et al. (2016).

Figure S4. Time series of forecasted and actual wind direction and wind speed. The whole campaing period from July 8th to 26th is shown.

Figure S5. Correlations of wind direction and wind speed between airborne measurement data and ECMWF forecast data. Correlation coefficients are abbreviated with Pr.

Figure S6. Biogenic CO_2 mixing ratios up- and downwind of Berlin on July 20th.

Figure S7. Ascents of a captive balloon system located at Tempelhofer Feld on July 24th. Wind measurements were carried out by the DWD (R. Becker, P. Stanislawsky, M. Koßmann) in the framework of the [UC]^2 project.

Figure S8. Backward trajectory calculations for July 24th. Trajectories were started at 14:30 UTC from the downwind flight track backwards in time for 6 hours. Colour coded is the height of the trajectory according to its relative position.

Figure S9. Population density for Berlin and the state Brandenburg from 2017. The yellow to red colours indicate the inhabitants per km^2, the blue dots show numbers for total population in each municipality. The Berlin city boundary (black) was added as well as latitude and longitude labels. Adapted after Strukturatlas Land Brandenburg (2017).

Figure S10. Curtain of simulated c-CH_4 and c-CO_2 on July 20th. The third crossing of the Berlin plume at ~1600 m altitude is shown from ~13:20 to ~13:35 UTC.

Figure S11. Time-series of the simulated c-CO_2 plume on July 24th. Shown are snapshots at (a) 14 UTC, which is identical to Fig. 10b and (b) at 16 UTC to indicate, that the plume moves towards the west during the afternoon.

Text S1. Calibration procedure and measurement uncertainty

Text S2. Greenhouse gas time series and altitude profiles

Text S3. ECMWF forecast data and wind measurement agreement

Text S4. Biogenic CO_2 flux

Text S5. Wind situation on July 24th

Text S6. Trajectories on July 24th

Text S7. Berlin and its surrounding area

Text S8. Simulated vertical GHG distribution within the PBL

Figures

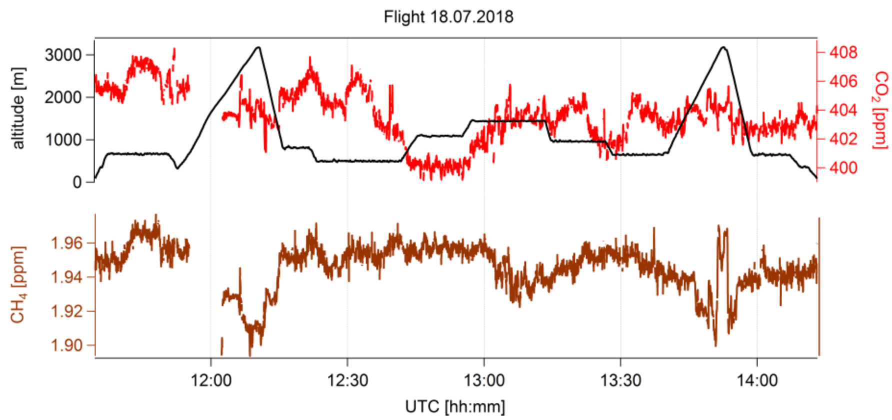
Flight 18.07.2018
altitude [m]
CO_2 [ppm]
CH_4 [ppm]
UTC [hh:mm]

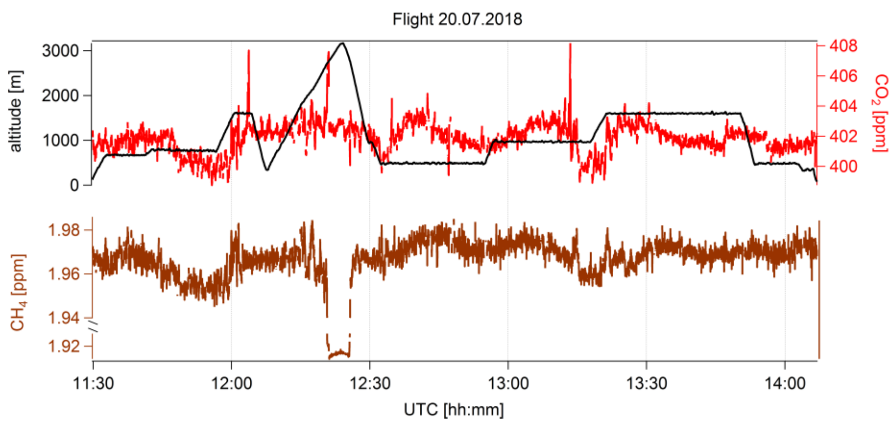
Flight 20.07.2018
altitude [m]
CO_2 [ppm]
CH_4 [ppm]
UTC [hh:mm]

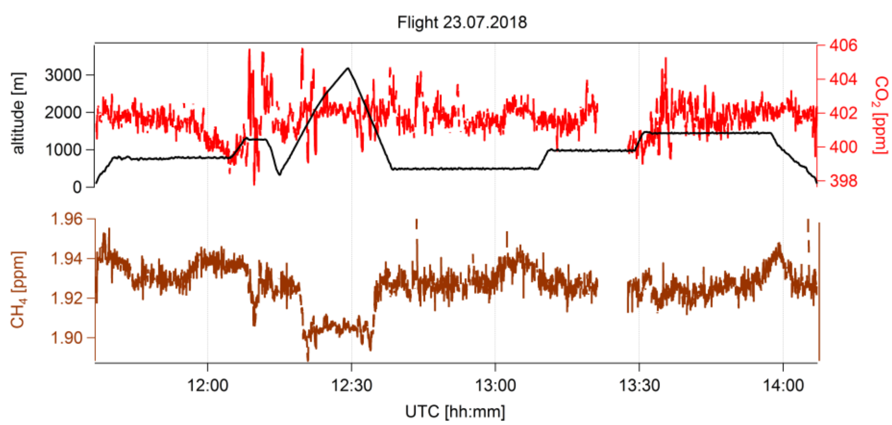
Flight 23.07.2018
altitude [m]
CO_2 [ppm]
CH_4 [ppm]
UTC [hh:mm]

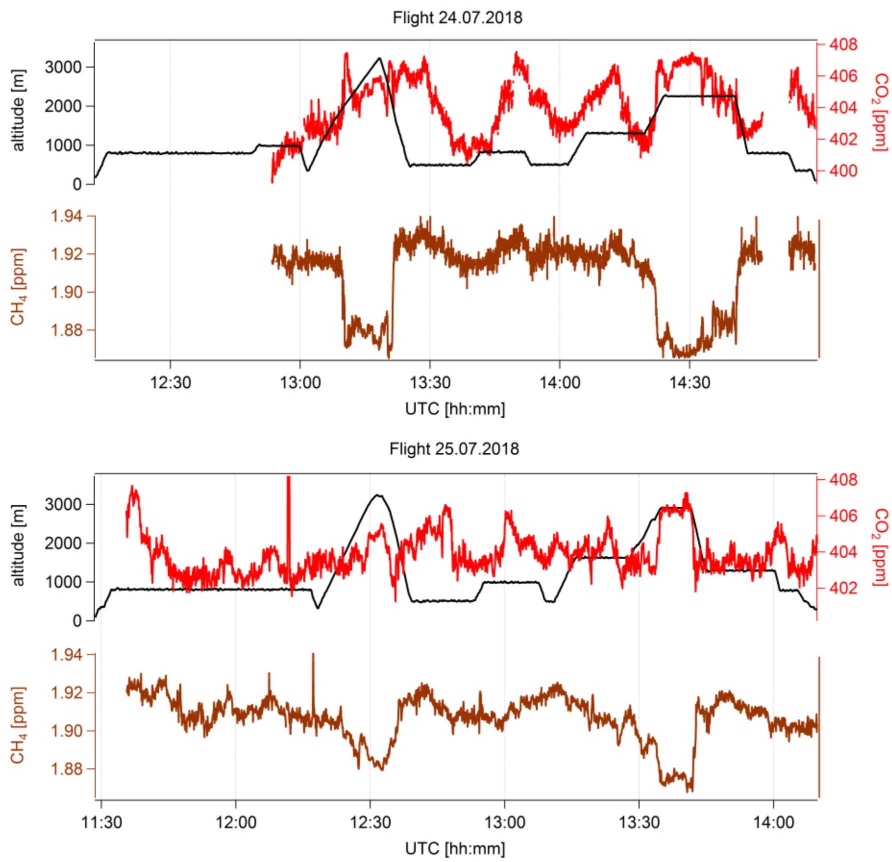

Figure S1. Time series of CO_2, CH_4 and flight altitude for five research flights during July 2018.

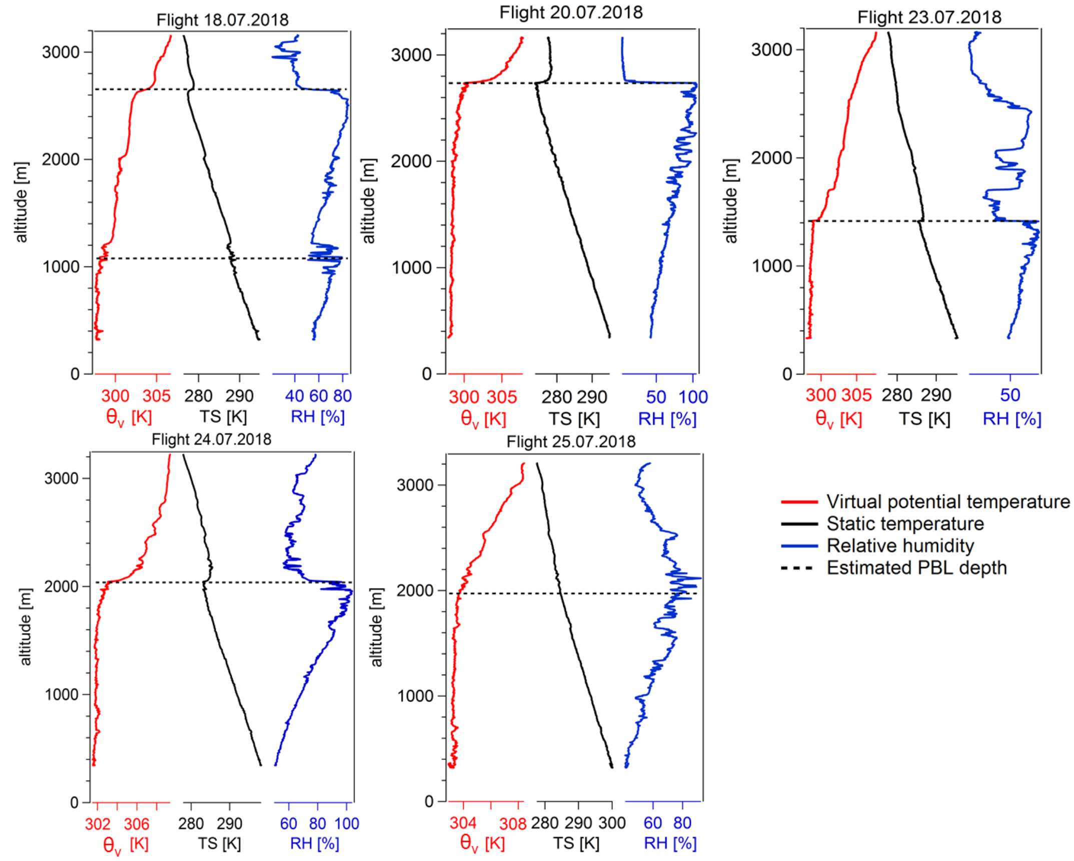

Figure S2. Vertical profiles of the upward spiral at Tempelhofer Feld. The PBL depth (dashed black line) was determined from virtual potential temperature, static temperature and relative humidity.

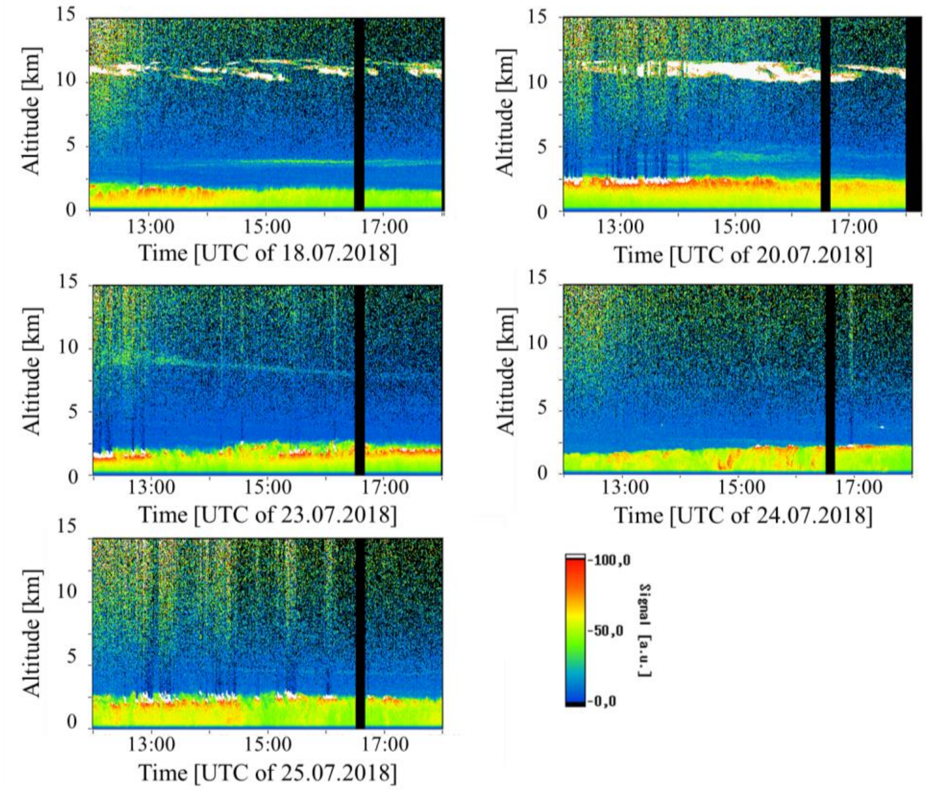

Figure S3. Aerosol lidar measurements at Leipzig. The temporal evolution of the range-corrected signal at 1064 nm is shown. Available at http://polly.tropos.de/?p=lidarzeit&Ort=1&Jahr=2018. Accessed October 04, 2019. Further information can be found in Engelmann et al. (2016) and Baars et al. (2016).

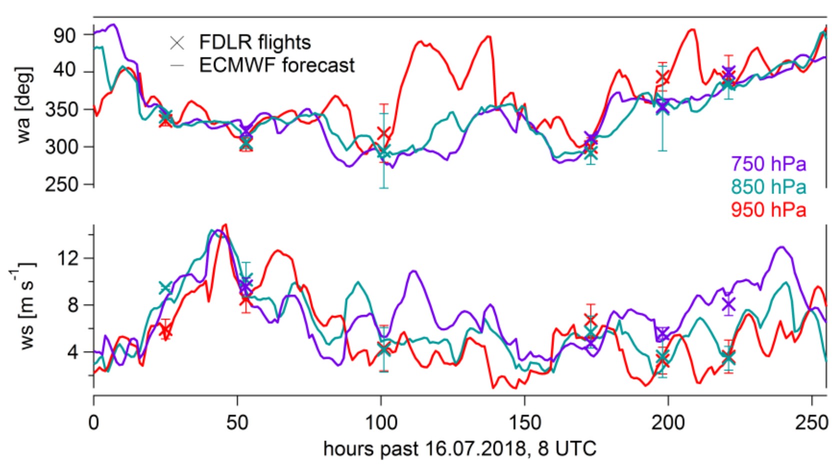

Figure S4. Time series of forecasted and actual wind direction and wind speed. The whole campaign period from .July 8th to 26th is shown.

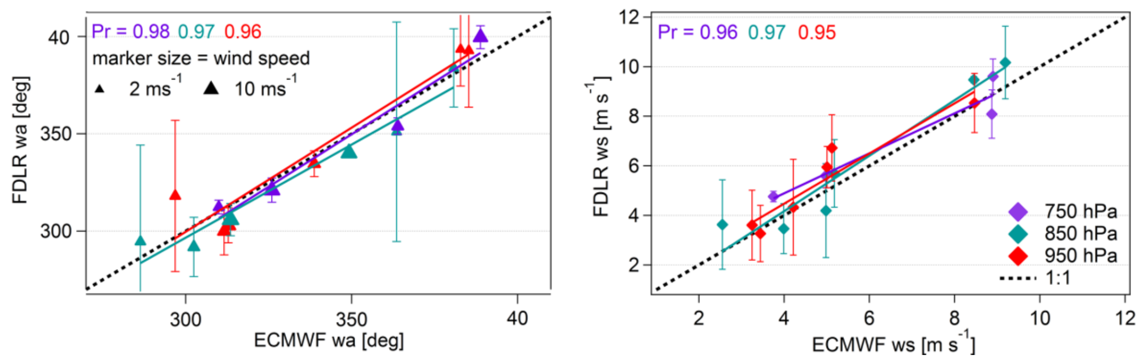

Figure S5. Correlations of wind direction and wind speed between airborne measurement data and ECMWF forecast data. Correlation coefficients are abbreviated with Pr.

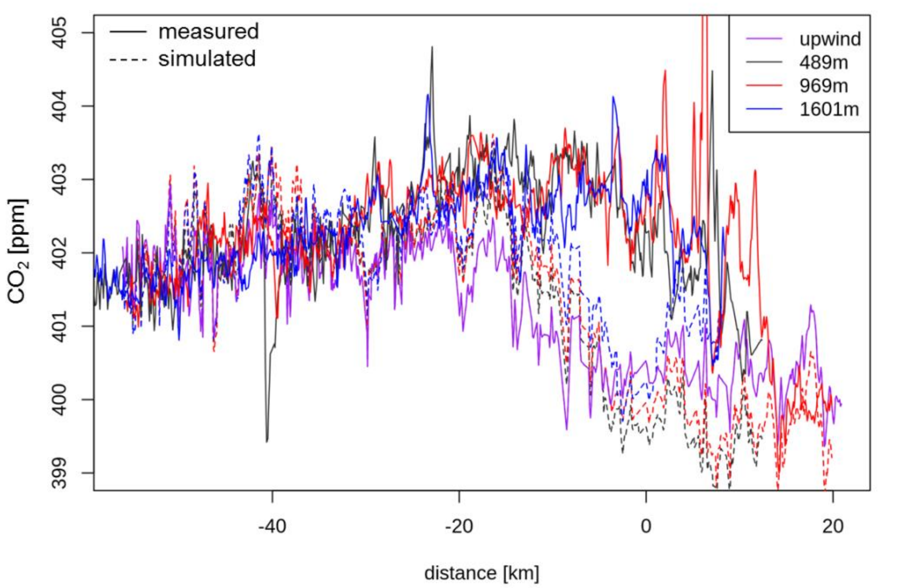

Figure S6. Biogenic CO_2 mixing ratios up- and downwind of Berlin on July 20th.

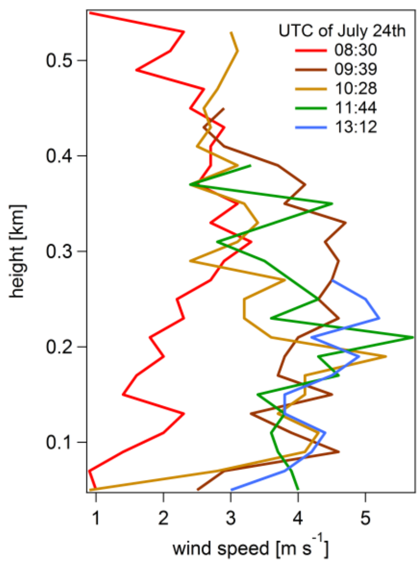

Figure S7. Ascents of a captive balloon system located at Tempelhofer Feld on July 24th. Wind measurements were carried out by the DWD (R. Becker, P. Stanislawsky, M. Koßmann) in the framework of the [UC]^2 project.

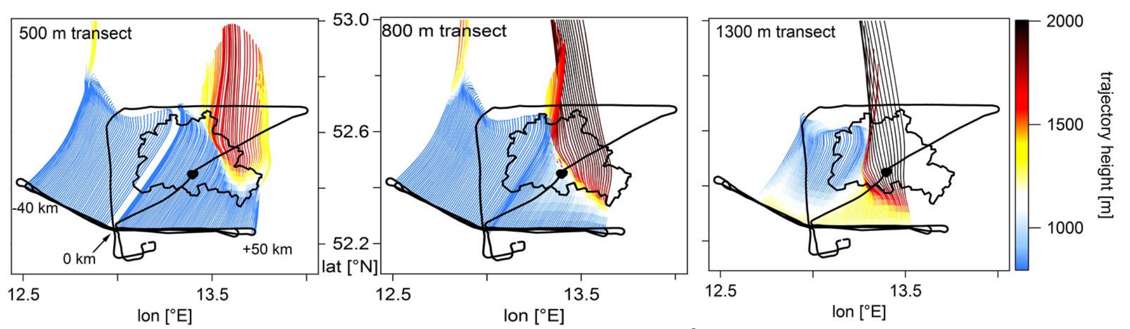

Figure S8. Backward trajectory calculations for July 24th. Trajectories were started at 14:30 UTC from the downwind flight track backwards in time for 6 hours. Colour coded is the height of the trajectory according to its relative position.

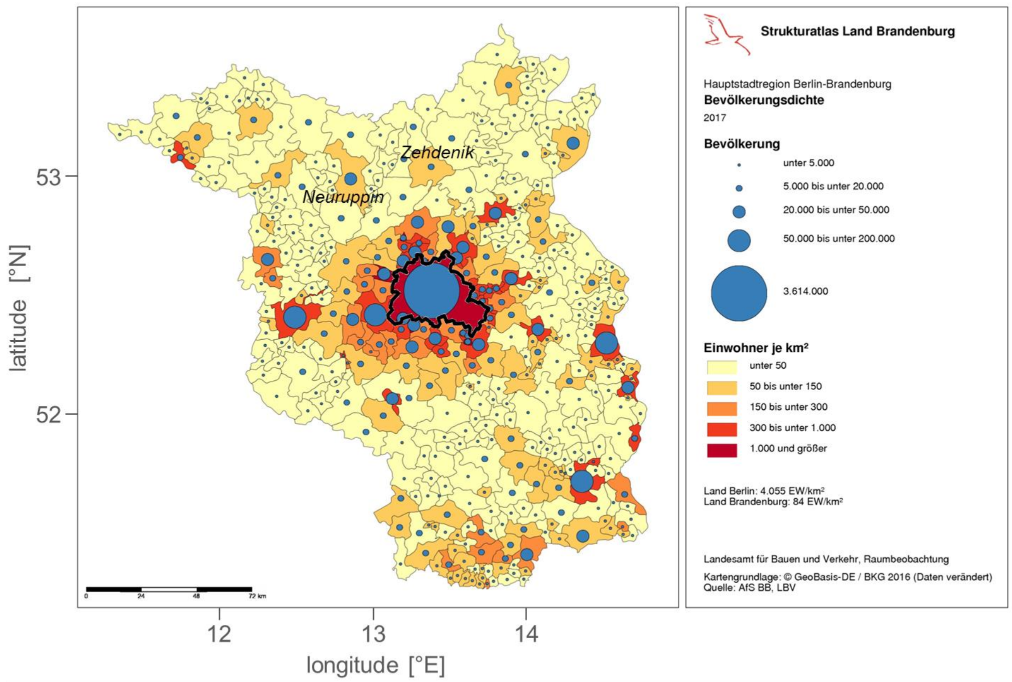

Figure S9. Population density for Berlin and the state Brandenburg from 2017. The yellow to red colours indicate the inhabitants per km^2, the blue dots show numbers for total population in each municipality. The Berlin city boundary (black) was added as well as latitude and longitude labels. Adapted after Strukturatlas Land Brandenburg (2017).

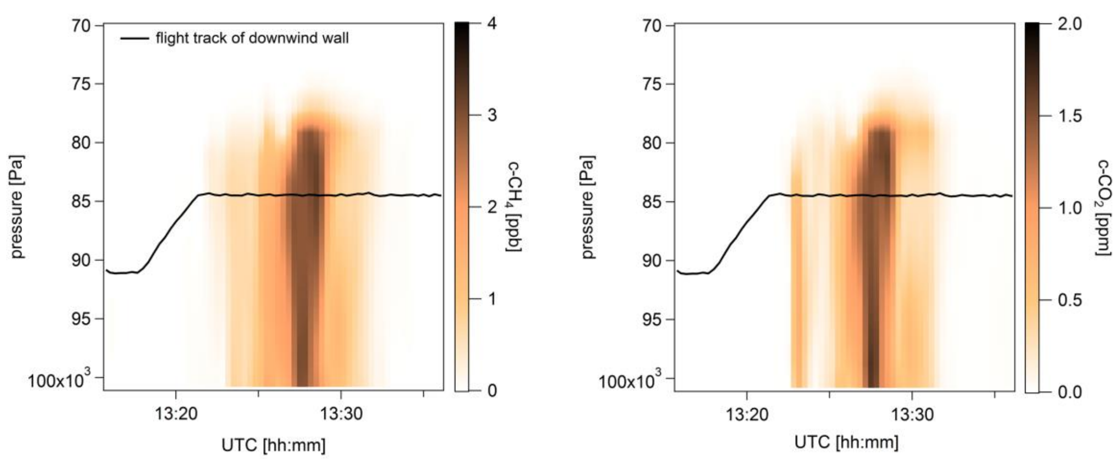

Figure S10. Curtain of simulated c-CH_4 and c-CO_2 on July 20th. The third crossing of the Berlin plume at ~1600 m altitude is shown from ~13:20 to ~13:35 UTC.

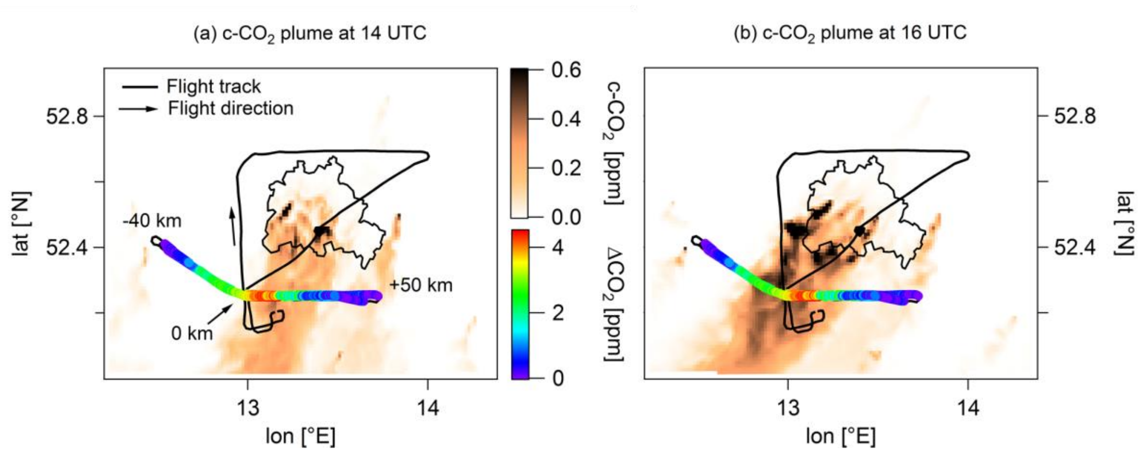

Figure S11. Time-series of the simulated c-CO_2 plume on July 24th. Shown are snapshots at (a) 14 UTC, which is identical to Fig. 10b and (b) at 16 UTC to indicate, that the plume moves towards the west during the afternoon.

Text

Text S1. Calibration procedure and measurement uncertainty

The Picarro analyser was frequently calibrated with four multi gas cylinders from Air Liquide (AL) containing the following CO_2 and CH_4 mixing ratios [ppm/ppb] in synthetic air: 777/1.795, 428.8/2.010, 411.8/1.824 and 369.2/1.607. The manufacturer states an uncertainty of ±2 %. The highest CO_2 mixing ratio of 777 ppm was however not used for the analysis as the operating range of the instrument is typically between 300 and 500 ppm, as stated in the Picarro Certificate of Compliance which comes with the purchase of the instrument. Prior and after the campaign the AL standards were calibrated against two NOAA multi gas standards (#CB11542 and #CB11361). Assuming the primary standards are the truth, the AL uncertainty of 2 % could therefore be reduced to <0.1 % for CO_2 and <0.4 % for CH_4. The total measurement uncertainty is determined to better than 0.2 ppm for CO_2 and 1.1 ppb for CH_4 based on the summation of the following sources of uncertainty in quadrature: (1) measurement precision: 1σ of 180 s mean of a 10 min calibration sequence (2) uncertainty associated with the water vapour correction: taken from Rella (2010) with a maximum measured water vapour mixing ratio of 2.2 % (3) drift of the instrument with time: taken from flight analyser data sheet (Picarro, 2009) with a maximum flight time of 2.5 hours (4) drift of the instrument with temperature: taken from the Picarro Certificate of Compliance with a maximum measured temperature difference of 15 °C (5) scale reproducibility of the primary standards: given is the 68^{th} percentile of the absolute values of the differences among all the pairs divided by the square root of two (6) scale reproducibility of the secondary standards.

Text S2. Greenhouse gas time series and altitude profiles

Time series for CO_2 (red), CH_4 (brown) and flight altitude (black) of each of the five performed research flights are presented in Fig. S1, where the GHG mixing ratios from the Picarro analyser are corrected according to the delay time of the instrument (~15 s). Altitude profiles of virtual potential temperature (θ_v, red), static temperature (ST, black), and relative humidity (RH, blue) are shown in Fig. S2. The PBL depth (dashed black line in Fig. S2) was determined considering the average of three different approaches (1) level of maximum gradient in virtual potential temperature ($d\theta_v/dz$), following Dai et al. (2014) (2) base level of an elevated temperature (static temperature) inversion and (3) level of minimum vertical gradient of relative humidity (dRH/dz), both following Seidel et al. (2010). PBL depths were cross verified through the comparison with aerosol lidar measurements at Leipzig, Germany, performed within EARLINET (European

Aerosol Research Lidar Network, Pappalardo et al., 2014; see Fig. S3). PBL heights retrieved from the ECMWF forecast data (averaged within 50.85 to 50.75 °N and 12.45 to 14.2 °E) were found to agree within ~250 m compared to the PBL height deduced from the airborne measurements.

Text S3. ECMWF forecast data and wind measurement agreement

We compare our airborne wind measurements (FDLR = aircraft call sign) to ECMWF forecast data, which are used as input for HYSPLIT trajectory calculations. To capture the characteristics of the whole PBL we consider three different pressure levels: 750, 850 and 950 hPa. Figure S4 presents the time series of ECMWF wind direction (wa, upper panel) and ECMWF wind speed (ws, lower panel) within the whole campaign period from 16th of July at 8 UTC to 26th of July at 23 UTC. The three different pressure levels are expressed as solid lines. Wind directions ranged from 270° to 100° with wind speeds from 1 to 15 m s^{-1}. Wind measurements on our flight days are indicated by crosses. Error bars are the deviation of the wind speed and wind direction as we calculated an average of the whole flight at pressure levels within ± 5 hPa of the given pressure height. Figure S5 shows the correlation between measured wind direction and wind speed on our flight days with ECMWF data. As the overall correlation (R = 0.95 to 0.98) is excellent, we take the ECWMF data as reliable fur further analysis. Note that the wind direction markers in Fig. S5 are sized according to the wind speed. Generally better agreement in wind direction was observed when wind speeds were higher.

Text S4. Biogenic CO_2 flux

Figure S6 shows the measured (solid lines) and simulated (dashed lines) CO_2 mixing ratios downwind of Berlin. The dashed lines represent the predicted result from WRF-GHG, simulating the biospheric CO_2 contribution using an online VPRM model driven by MODIS indices (Mahadevan et al., 2008). Here we analyse the signals predicted by the biosphere if only biogenic uptake was considered (i.e. assuming complete absence of anthropogenic sources). The mixing ratios were derived from the simulation by replacing the upwind-simulated mixing ratios of the WRF base reference by the actual upwind CO_2 measurements. Next, the simulated downwind mixing ratios were corrected by that estimated bias. Therefore, the upwind measured and simulated CO_2 mixing ratios are equal by definition and only depicted by the solid light purple line. Variation in the predicted dashed concentrations corresponds to changes of biospheric-only CO_2 mixing ratios at respective downwind measurement locations. At the edges of our flight track, which we assume represent the atmospheric background, the model matches the measured CO_2 pattern quite well, which leads us to believe that its predictions are accurate.

As can be seen, the influence of the biosphere between upwind and downwind legs of the flight is predicted to be small and well within the variability of the measurements. On top of that, the change of the modeled signal inside the constrained area is variable with both altitude and distance (as defined on x-axis), reflecting the influence of vertical transport dynamics inside the PBL superimposed on regional-scale variability of the predicted tracer fields. For the lowest leg the strongest uptake of CO_2 is estimated, however the surface-driven influence of biosphere gets less intense towards the higher flight altitudes. In turn, regional scale variability causes the relation between upwind and downwind simulations to be negative (distances between approx. 0 km to 20 km) or positive (-20 km to -10 km), depending on the horizontal location.

This variability in horizontal and vertical direction makes it difficult to accurately quantify the overall biogenic influence without adding an extra layer of complexity to the applied method. In fact, even if it were to be applied, we believe that the correction of the estimated anthropogenic flux would be very minor, as the difference in the mixing ratios between the upwind leg and the simulated downwind legs within the city plume is usually not larger than 0.5 ppm. The estimated enhancement from the city of ~4 ppm (which corresponds to an anthropogenic flux of 1.39 ± 0.76 t CO_2 s^{-1}) would be only slightly altered if a vertically-weighted mean of simulated concentrations was used as background instead of upwind measurement. On top of that, the uncertainty of such estimation would be difficult to quantify without a detailed analysis of the modeled output.

It should also be noted that our estimates of the biogenic signals are potentially offset over the sections of the transects immediately downwind of the Berlin urban area. This is caused by misrepresentation of the urban biosphere in VPRM, as the driving MODIS indices cannot accurately discern the urban biosphere from other land use types within the city boundary due to insufficient spatial coverage. To properly account for the biogenic CO_2 signal, modifications to the VPRM system would be required, potentially in a manner similar to the one adopted by Hardimann et al. (2017).

Therefore, based on the available data, we deem it unnecessary to correct for the biogenic influence explicitly, and conservatively estimate that the anthropogenic emissions would not be enlarged by more than ~12 % if the biogenic uptake were to be considered. This number, corresponding to the total CO_2 biogenic flux in the constrained area, is conservative, and well within the overall uncertainty of calculated anthropogenic flux.

The modeling system used in this study was the same that was used for simulations preformed in the scope of the CoMet 1.0 (Carbon Dioxide and Methane Mission). The setup consisted of a WRF-Chem v3.9.1.1. model (Skamarock et al, 2008) run with the GHG option enabled for a European-wide L60 10 km x 10 km domain with a nested L60 2 km x 2 km domain centered over Berlin. Meteorology was driven by the ERA5 product from Copernicus Climate Change Service (C3S, 2017). More details about the system setup can be found in Galkowski et al. (in prep).

Text S5. Wind situation on July 24th

Calm winds during the night and in the morning were recorded by seven ground based measurement stations within and around Berlin (http://wind.met.fu-berlin.de/wind/archiv/form.php), however the wind speed increased dependent on the location between 6 and 9 UTC. This rise of low level winds (<400 m) in the morning is further in agreement with five ascents of a captive balloon system located at Tempelhofer Feld. Measurements were performed by the DWD within the $[UC]^2$ project, the data were processed and provided by R. Becker, P. Stanislawsky and M. Koßmann. Figure S7 shows that the average wind speed at 08:30 UTC was only 2.2 ± 0.7 m s^{-1}, however it was strongly rising to 3.9 ± 0.7 m s^{-1} already at 9:39 UTC. Additional balloon ascents afterwards (at 10:28, 11:44 and 13:12 UTC) show similar and relatively consistent wind speeds (3.3 ± 0.9, 3.8 ± 0.7 and 4.3 ± 0.6 m s^{-1}, respectively). Our downwind wall is approximately 30 to 40 km downwind of the city centre, hence with an averaged measured wind speed during the flight of 3.6 m s^{-1}, the air masses would have needed three hours to travel from the city centre towards our flight path. Thus it is uncertain whether the accumulation due to calm winds was already swiped away or not.

Text S6. Trajectories on July 24th

Figure S8 displays backward trajectory calculations being started from the three transects within the PBL at 14:30 UTC. Colour coded is hereby the height of the trajectory. Note that all calculations reach 6 h backward in time, thus the accumulation of air masses in the western part of the plume is visible (the right part of the trajectories is distinguishable from the left part due to their plume age), which is consistent with the observed change in GHG mixing ratios as depicted in Fig. 10a of the main paper. Further the trajectories do not exhibit a similar picture in the different heights within the PBL (500, 800 and 1300 m transect), which is however contradictory to the uniformly observed GHG mixing ratios at all heights (see also Fig. 10a). Thus, assessing the uncertainty of the background, where we would use the upwind CO_2 and CH_4 measurement data, is not feasible.

Text S7. Berlin and its surrounding area

Figure S9 shows the population density for Berlin and the surrounding state Brandenburg from 2017. The caption is only available in German, however the yellow to red colours indicate the inhabitants per km^2 and the blue dots show numbers for total population in each municipality. The Berlin city boundary (black) was added as well as latitude and longitude labels for better orientation. It is obvious, that Berlin has a higher population density compared to its surrounding (4055 vs. 84 inhabitants per km^2) and seems therefore to be relatively isolated. Northwest of the city (i.e. upstream of the flight track on July 20th) two municipalities (Neuruppin and Zehdenik) are located, but only with a population density of 50 to 100 inhabitants per km^2. To the west and east of these small cities large nature parks are located (Naturpark Westhavelland, Biosphärenreservat Schorfheide-Chorin).

Text S8. Simulated vertical GHG distribution within the PBL

The PBL on July 20th extends from the surface up to ~2700 m, as indicated by meteorological measurements. The part of the plume between ~300 and ~1600 m was sampled by the aircraft; however the lowest ~300 m were not accessible due to flight restrictions over the city. To still account for the distribution of GHG from the surface towards the top of the PBL we analyse the vertical plume structure using the MECO(n) model. Figure S10 shows for the third crossing of the Berlin plume at ~1600 m the simulated c-CH_4 and c-CO_2 mixing ratios in the vertical. Between the surface and the top of the PBL the plume is not lofted or depicts any vertical structures. Therefore our assumption of a well-mixed PBL is valid.

References

Baars, H. et al. 2016. An overview of the first decade of PollyNET: an emerging network of automated Raman-polarization lidars for continuous aerosol profiling. *Atmos Chem Phys* **16**: 5111–5137, DOI: 10.5194/acp-16-5111-2016.

C3S Copernicus Climate Change Service: ERA5: Fifth generation of ECMWF atmospheric reanalyses of the global climate. Copernicus Climate Change Service Climate Data Store (CDS), https://cds.climate.copernicus.eu/cdsapp#!/home, 2017.

Dai, C, Wang, Q, Kalogiros, JA, Lenschow, DH, Gao, Z, Zhou, M. 2014. Determining Boundary-Layer Height from Aircraft Measurements. *Bound-Lay Meteorol* **152(3):** 277–302, DOI: 10.1007/s10546-014-9929-z.

Engelmann, R, Kanitz, T, Baars, H, Heese, B, Althausen, D, Skupin, A, Wandinger, U, Komppula, M, Stachlewska, IS, Amiridis, V, Marinou, E, Mattis, I, Linné, H, and Ansmann, A. 2016. The automated multiwavelength Raman polarization and water-vapor lidar Polly^{XT}: the neXT generation. *Atmos Meas Tech* **9**: 1767–1784, DOI: 10.5194/amt-9-1767-2016.

Hardiman, BS, Wang, JA, Hutyra, LR, Gately, CK, Getson, JM, Friedl, MA. 2017. Accounting for urban biogenic fluxes in regional carbon budgets. *The Science of the total environment* **592:** 366-372, DOI: 10.1016/j.scitotenv.2017.03.028.

Mahadevan, P, Wofsy, SC, Matross, DM, Xiao, X, Dunn, AL, Lin, JC, Gerbig, C, Munger, JW, Chow, VY, Gottlieb, EW. 2008. A satellite-based biosphere parameterization for net ecosystem CO_2 exchange: Vegetation Photosynthesis and Respiration Model (VPRM). *Global Biogeochem Cy* **22(2)**, DOI: 10.1029/2006GB002735.

Pappalardo, G, Amodeo, A, Apituley, A, Comeron, A, Freudenthaler, V, Linné, H, Ansmann, A, Bösenberg, J, D'Amico,G, Mattis, I, Mona, L, Wandinger, U, Amiridis, V, Alados-Arboledas, L, Nicolae, D, Wiegner, M. 2014. EARLINET: towards an advanced sustainable European aerosol lidar network. *Atmos Meas Tech* **7**: 2389–2409, DOI: 10.5194/amt-7-2389-2014.

Picarro, 2009. Picarro G1301-m CO_2/CH_4/H_2O Flight Analyzer. Available at https://www.picarro.com/assets/docs/CO2_CH4_flightanalyzer_datasheet.pdf. Accessed October 01, 2019.

Rella, C. Accurate Greenhouse Gas Measurements in Humid Gas Streams Using the Picarro G1301 Carbon Dioxide / Methane / Water Vapor Gas Analyzer, 2010. Available at https://www.picarro.com/assets/docs/White_Paper_G1301_Water_Vapor_Correction.pdf. Accessed October 01, 2019.

Seidel, DJ, Ao, CO, Li, K. 2010. Estimating climatological planetary boundary layer heights from radiosonde observations: Comparison of methods and uncertainty analysis. *J Geophys Res* **115(D16):** 123, DOI: 10.1029/2009JD013680.

Skamarock, WC, Klemp, JB, Dudhia, J, Gill, DO, Barker, DM, Duda, MG, Huang, X-Y, Wang, W, Powers, JG. 2008. A Description of the Advanced Research WRF Version 3. NCAR Tech. Note NCAR/TN-475+STR, 113 pp. DOI: 10.5065/D68S4MVH.

Strukturatlas Land Brandenburg (2017), plot retrieved from an interactive tool on http://strukturatlas.brandenburg.de/. Accessed January 22, 2020.

Acknowledgements

Authors acknowledge data provision by the PollyNET team in the frame of ACTRIS (ACTRIS-2 under grant agreement no. 654109 from the European Union's Horizon 2020 research and innovation programme).